# Single- and double-electron processes in collisions of $Xe^{23+}$ ions with helium

Baowei Ding,[1,*] Deyang Yu,[2,†] Fangfang Ruan,[2] Rongchun Lu,[2] Caojie Shao,[2,3] Chengliang Wan,[1] Shangwen Chen,[1] and Xiaohong Cai[2]

[1]*School of Nuclear Science and Technology, Lanzhou University, Lanzhou 730000, People's Republic of China*

[2]*Institute of Modern Physics, Chinese Academy of Science, Lanzhou 730000, People's Republic of China*

[3]*Graduate School of the Chinese Academy of Sciences, Beijing 100049, People's Republic of China*

(Received 29 May 2010; published 9 September 2010)

We report the measurements of relative cross sections for single capture (SC), double capture (DC), single ionization (SI), double ionization (DI), and transfer ionization (TI) in collisions of $Xe^{23+}$ ions with helium atoms in the velocity range of 0.65–1.32 a.u. The relative cross sections show a weak velocity dependence. The cross-section ratio of double- (DE) to single-electron (SE) removal from He, $\sigma_{DE}/\sigma_{SE}$, is about 0.45. Single capture is the dominant reaction channel which is followed by transfer ionization, while only very small probabilities are found for pure ionization and double capture. The present experimental data are in satisfactory agreement with the estimations by the extended classical over-barrier (ECB) model.

DOI: 10.1103/PhysRevA.82.032703 PACS number(s): 34.70.+e, 34.50.Fa

## I. INTRODUCTION

Highly charged ions (HCI's) colliding with atoms is an intense field of atomic-collision research. The reasons range from its fundamental importance in understanding the complicated ion-atom reactions, testing the theoretical models [1–3] to their significant applications on plasma physics [4], and stellar atmospheres [5]. In the past few decades people have developed a coincidence technique, through which the charge states of both the projectile and the target could be measured simultaneously. In the case of $Xe^{23+}$ impacting on a helium atom, five possible charge-changing processes are listed below

$$Xe^{23+} + He \rightarrow \begin{cases} Xe^{22+} + He^{+} & \text{single capture (SC)} \\ Xe^{23+} + He^{+} + e^{-} & \text{single ionizaition (SI)} \\ Xe^{23+} + He^{2+} + 2e^{-} & \text{double ionizaition (DI)} \\ Xe^{21+} + He^{2+} & \text{double capture (DC)} \\ Xe^{22+} + He^{2+} + e^{-} & \text{transferionization (TI)} \end{cases} \quad (1)$$

According to the number of electrons removed from He, these five reactions can be divided into two groups: single- (SE) and double-electron (DE) processes (i.e., SE = SC + SI and DE = DI + DC + TI). The DE process, in particular, provides an important test for the four-body theories.

At very low impact velocities ($v_p \ll 1$ a.u.), electron capture is so dominant that ionization can be neglected. On the contrary, at very high impact velocities ($v_p \gg 1$ a.u.), ionization is the dominant process. In the two velocity ranges mentioned above, the reaction channels are relatively homogeneous and a number of measurements [6–11] have been carried out in collisions of HCI's with helium atoms. However, in the overlap region ($v_p \sim 1$ a.u.), the ionization involving HCI's is not a weak process any more. As a result, a large number of reaction channels are involved and a full quantum-mechanical treatment becomes prohibitively difficult. At the same time, measurements [12,13] as well as their support toward the theoretical investigation are still relatively scarce.

In this work, we have carried out the measurements of relative cross sections for $Xe^{23+}$+ He collisions, using coincidence techniques, in the velocity range of 0.65–1.32 a.u. The objectives of this work are to study the velocity dependencies and the relative importance of various reaction channels. Atomic units are used throughout the work, unless otherwise indicated.

## II. EXPERIMENTAL METHOD

The experiments were carried out on the high-voltage-electron-cyclotron-resonance ion source (HV-ECRIS) at the Institute of Modern Physics (IMP), Chinese Academy of Science (CAS). The experimental arrangement is schematically drawn in Fig. 1. In brief, a $Xe^{23+}$ ion beam exacted from the HV-ECRIS was analyzed by the magnet to a desired energy and charge state. Then the beam was focused by the magnetic quadrupole lens, collimated to $0.5 \times 0.5$ mm$^2$ by means of two sets of slits and guided into a vacuum chamber in which base pressure was of the order of $10^{-6}$ Pa. The typical $Xe^{23+}$ ion beam current was 10 pA. The target gas was introduced through a needle which was perpendicular to the beam direction. The working pressure in the gas cell was maintained at $1 \times 10^{-4}$ Pa to avoid double collisions within the target region. The ion beam then interacted with an effusive gas target. The charge states of projectiles leaving the cell after the collision were analyzed by an electrostatic deflector and the projectiles then were detected by a position-sensitive microchannel plate (PS-MCP) detector. An electric field extracted the recoil ions ($He^{+}$ and $He^{2+}$) produced with low kinetic energy and a time-of-flight spectrometer (TOFS) was used to determine their charge states. After acceleration, the recoil ions drifted in a field-free tube to be focused in time and then impacted on the recoil microchannel plate (R-MCP) detector with a 36 mm diameter. Due to the high acceleration voltage (3 kV) before the recoil

*dingbw@lzu.edu.cn, dingbw2002@yahoo.com.cn

†d.yu@impcas.ac.cn

 

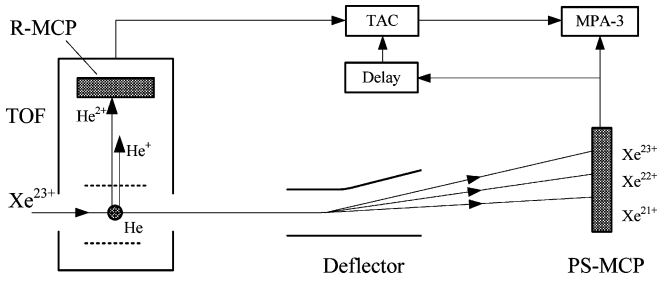


FIG. 1. Scheme of experimental arrangement.

ions arriving at R-MCP, the detection efficiency of the recoil ions is close to unity, and the efficiency difference between $He^+$ and $He^{2+}$ can be neglected. The time of flight (TOF) of recoil ions from reaction center to R-MCP detector is characteristic for their $m/q$ ratios, where $m$ and $q$ are the mass and charge of a recoil ion, respectively. The flight time was measured with a time-amplitude converter (TAC) which was started by the fast signal from the R-MCP and stopped by the delayed one from PS-MCP. Figure 2(a) shows a TOF spectrum for $He^+$ and $He^{2+}$ induced by 38.5-keV/u $Xe^{23+}$ beam. As can be seen, the charge states of interest could easily be separated. The TOF spectrum was automatically correlated to the position spectrum of the scattered projectiles. Finally, we got the two-dimensional position-versus-TOF spectrum, which allowed the identification of various reaction channels. A two-dimensional spectrum for the case of 38.5-keV/u $Xe^{23+}$ impact is shown in Fig. 2(b), in which the columns labeled with $Xe^{23+}$, $Xe^{22+}$, and $Xe^{21+}$ denote the results for projectiles undergoing no charge change, single- and double-electron capture, respectively, and the rows labeled

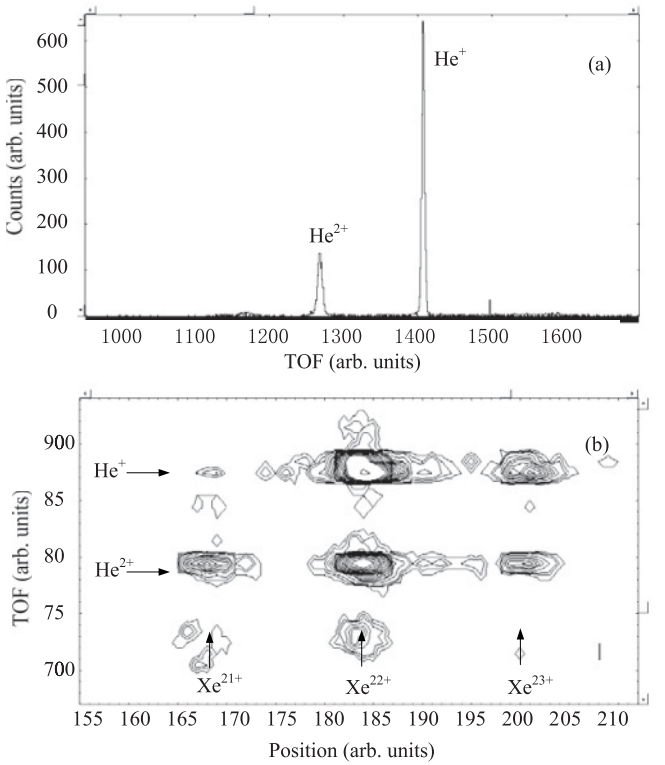


FIG. 2. (a) Time-of-flight spectrum and (b) two-dimensional coincidence spectrum for 38.5-keV/u $Xe^{23+}$+ He collisions.

with $He^+$ and $He^{2+}$ denote the data for He atoms undergoing single- and double-electron loss, respectively. As seen from Fig. 2(b), five reaction channels expressed in (1) are distinguished.

The mainly possible uncertainties of experimental ratios come from the efficiency of R-MCP detector (<10%), multicollision (<3%), determining the counting region in the two-dimensional spectrum (<10%) and statistical errors which are within 5%. Full details of the error analysis have been given in our previous paper [14,15].

## III. RESULTS AND DISCUSSION

We have performed the measurements for $Xe^{23+}$+ He collisions in the velocity range from 0.65 to 1.32 a.u. Since $He^+$ and $He^{2+}$ can be formed through the SE (SC and SI) and DE (DI, DC, and TI) processes, respectively, it is a common and effective way in understanding the ion-atom collision process to analyze the relative cross-section ratios, such as $\sigma_{DE}/\sigma_{SE}$, $\sigma_{SC}/(\sigma_{SE}+\sigma_{DE})$, $\sigma_{SI}/(\sigma_{SE}+\sigma_{DE})$, $\sigma_{DI}/(\sigma_{SE}+\sigma_{DE})$, $\sigma_{DC}/(\sigma_{SE}+\sigma_{DE})$, $\sigma_{TI}/(\sigma_{SE}+\sigma_{DE})$, and so forth. In Fig. 3 our measured cross-section ratios are displayed as a function of the projectile velocity. The general shape for ratios roughly shows a velocity-independence behavior, which disagrees with the results [16] by ions with very low charge states in the same energy range. This indicates changes of the projectile velocity play little role on the charge transfer and the ionization relative to that caused by the strong Coulomb potential of HCI's at the present velocities. As can be seen from Fig. 3 ratios are clearly different for various reaction channels. For instance, $\sigma_{DE}/\sigma_{SE}$ is round 0.45, which is approximately the same with the results for ~0.16 a.u. $Xe^{23+}$+ He collisions by Andersson *et al.* [6]. For specific channels, collisions are dominated by SC, while DI is the least likely channel. One can see that the ratio $\sigma_{SC}/(\sigma_{SE}+\sigma_{DE})$ reaches 0.63 which is an order of magnitude larger than the sum of $\sigma_{SI}/(\sigma_{SE}+\sigma_{DE})$ and $\sigma_{DI}/(\sigma_{SE}+\sigma_{DE})$. The cross-section ratio $\sigma_{SI}/(\sigma_{SE}+\sigma_{DE})$ is only about 0.05 which is roughly equal to the ratio $\sigma_{DC}/(\sigma_{SE}+\sigma_{DE})$. The second most likely channel is TI whose relative cross section $\sigma_{TI}/(\sigma_{SE}+\sigma_{DE})$ is around 0.24. In collisions of HCI's with He, both electrons of the target may be captured into the excited states of the projectile. The double electrons in the excited states usually decay through two pathways: radiative stabilization and autoionization, which contribute to DC and transfer ionization, respectively. These two reactions can be described as

$$\begin{aligned} Xe^{23+} + He &\rightarrow Xe^{21+**} + He^{2+} \\ &\rightarrow \begin{cases} Xe^{21+} + He^{2+} + \gamma & (DC) \\ Xe^{22+} + He^{2+} + e^- & (TI) \end{cases}. \end{aligned} \tag{2}$$

However, in the present experiment, we cannot pick out these two channels, but only provide the total DC and TI cross sections.

Since the cross sections of pure ionization are very small in the present velocity range it is possible to estimate the total SE and DE cross sections within the frame of the classical over-barrier (COB) model [3]. According to the COB model the $m$th electron of the target is assumed to be released at

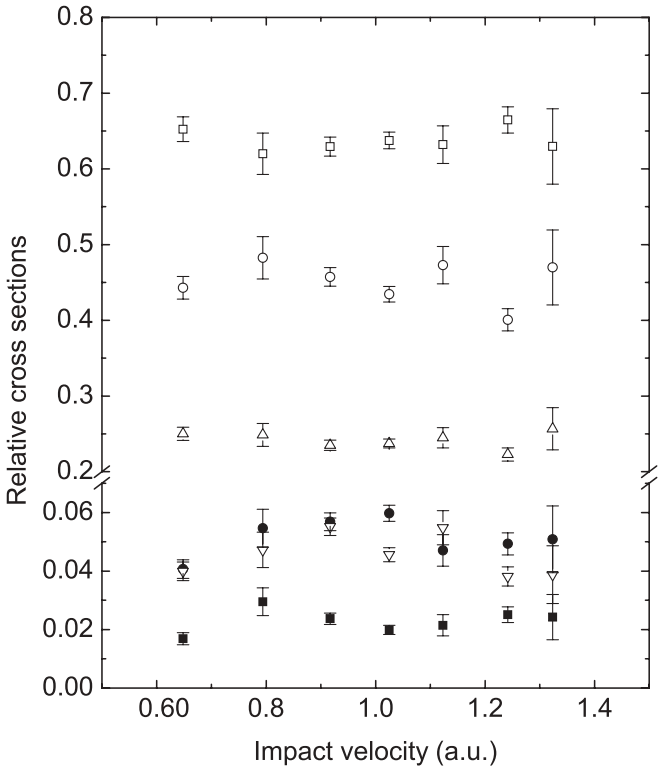


FIG. 3. Measured relative cross sections for $Xe^{23+}$ + He collisions. $\sigma_{DE}/\sigma_{SE}$ (○), $\sigma_{SC}/(\sigma_{SE}+\sigma_{DE})$(□), $\sigma_{TI}/(\sigma_{SE}+\sigma_{DE})$ (△), $\sigma_{DC}/(\sigma_{SE}+\sigma_{DE})$ (▽), $\sigma_{SI}/(\sigma_{SE}+\sigma_{DE})$ (●), and $\sigma_{DI}/(\sigma_{SE}+\sigma_{DE})$ (■).

a certain internuclear distance where its energy equals the saddle-point potential. This critical distance $R_{r,m}$ is given by

$$R_{r,m} = \frac{m + 2\sqrt{m(q-m+1)}}{|I_m|}, \tag{3}$$

where $I_m$ is the ionization potential that the target nuclear exerts on the $m$th electron. Using the absorbing sphere concept and assuming that no electron is recaptured by the target, one can estimate a cross section $\sigma_m$ for removing the $m$th electron from the target

$$\sigma_m = \pi\left(R_{r,m}^2 - R_{r,m+1}^2\right). \tag{4}$$

In the case of the helium target,

$$\sigma_{SE} = \sigma_1 = \pi\left(R_{r,1}^2 - R_{r,2}^2\right), \tag{5}$$

$$\sigma_{DE} = \sigma_2 = \pi R_{r,2}^2. \tag{6}$$

In collisions of $Xe^{23+}$ with He ($|I_1| = 0.903$ and $|I_2| = 2$), according to Eqs. (3), (5), and (6) the estimated $\sigma_{DE}/\sigma_{SE}$ approaches 0.73, which is much larger than the 0.45 of our measured value. The earlier investigation [7,17] proposed the transfer-excitation (TE) mechanism, which occurs at impact parameters smaller than a critical value $R_{TE}$, to be an explanation for low $\sigma_{DE}/\sigma_{SE}$ ratios. In the TE process two target electrons are transferred to the projectile followed by the recapture of the "inner" of these two electrons to an excited state of the target. This process is described as

$$Xe^{q+} + He \rightarrow Xe^{(q-2)+**} + He^{2+} \rightarrow Xe^{(q-1)+}He^{+*}. \tag{7}$$

Obviously, the TE process has the same final projectile and target charge state as SC. That is to say, it gives a net removal of only one target electron instead of double electrons. Following Cederquist [17] we modify Eqs. (5) and (6) by inclusion of the transfer-excitation process

$$\sigma_{SE} = \pi\left(R_{r,1}^2 - R_{r,2}^2 + R_{TE}^2\right), \tag{8}$$

$$\sigma_{DE} = \pi\left(R_{r,2}^2 - R_{TE}^2\right). \tag{9}$$

$R_{TE}$ is approximately given by

$$R_{TE}(n) = \frac{R_{r,2}}{1 + E_{ex}(n)R_{r,2}/(q-3)}, \tag{10}$$

where $n$ and $E_{ex}(n)$ are the principal quantum number and the corresponding excitation energy of the target after the electron transfer. $R_{TE}$ takes a maximum value when $n = 2$, while the minimum value is given by $n \rightarrow \infty$. For the He target, $R_{TE}(n \rightarrow \infty) = \frac{R_{r,2}}{1+2R_{r,2}/(q-3)}$. Collisions for the impact parameter $b < R_{TE}(n \rightarrow \infty)$ contribute to $\sigma_{SE}$ instead of $\sigma_{DE}$. Using the modified cross sections, we obtain the ratio $\sigma_{DE}/\sigma_{SE}$ to be about 0.4 which is in agreement with our experimental results.

Because TI is one of the important channels at the present velocities, it is unfeasible to discuss the specific reaction channel without taking the ionization process into account. At $R_{r,m}$ the $m$th electron moves in the joint potential well of the projectile and the target. This electron is called the quasimolecular electron. Due to the Stark shift its energy level $E_m$ becomes more strongly bound $E_m = -\frac{q}{R_{r,m}} - |I_m|$. For simplicity, it is supposed that the released electron only faces two choices: capture and ionization. We assume that ionization of the $m$th electron occurs when the Stark-shifted energy gained by this electron exceeds its total energy in the quasimolecular state. That is, $-\frac{q}{R_m} < -\frac{q}{R_{r,m}} - |I_m|$, where $R_m$ is the internuclear distance. From this the maximum distance $R_{i,m}$ at which ionization of the $m$th electron is possible can be obtained as

$$R_{i,m} = \frac{q}{\frac{q}{R_{r,m}} + |I_m|}. \tag{11}$$

As discussed previously, Eqs. (3) and (11) suggest that both $R_{r,m}$ and $R_{i,m}$ are independent of the projectile velocity. Usually, we should take the projectile-velocity effect on cross sections into account. However, in view of the velocity independencies of experimental data and also for simplicity, the influence of the projectile velocity can be neglected reasonably. Therefore, for example, the release probability of one target electron depends on the distance that the projectile travels within the circle with radius $R_{r,m}$. As a result, the release probability $P_{r,m}(b,q)$ at the impact parameter $b < R_{r,m}$ for the $m$th electron of the target is given by

$$P_{r,m}(b,q) = 2\sqrt{R_{r,m}^2(q) - b^2}(b < R_{r,m}). \tag{12}$$

Similarly, when $b < R_{i,m}$, we have

$$P_{i,m}(b,q) = 2\sqrt{R_{i,m}^2(q) - b^2}(b < R_{i,m}), \tag{13}$$

where $P_{i,m}(b,q)$ represents the ionization probability of the $m$th target electron. The probabilities are calculated using the unitarized formula

$$P_{\mathrm{ur},m}(b,q) = 1 - e^{-p_{r,m(b,q)}}(b < R_{r,m}), \tag{14}$$

$$P_{\mathrm{ui},m}(b,q) = \frac{p_{i,m}(b,q)}{p_{r,m}(b,q)} P_{\mathrm{ur},m}(b,q)(b < R_{i,m}), \tag{15}$$

$$P_{\mathrm{uc},m}(b,q) = P_{\mathrm{ur},m}(b,q) - P_{\mathrm{ui},m}(b,q)(b < R_{r,m}), \tag{16}$$

where $P_{\mathrm{ur},m}(b,q)$, $P_{\mathrm{ui},m}(b,q)$, and $P_{\mathrm{uc},m}(b,q)$ are the unitarized probabilities for the release, ionization, and capture, respectively. Within the independent electron approximation (IEA) and in the case of collisions of helium target, the cross-section expressions for various channels are written as

$$\sigma_{\mathrm{SE}} = 2\pi \int bdb[P_{\mathrm{ur},1}(1 - P_{\mathrm{ur},2}) + P_{\mathrm{ur},2}(1 - P_{\mathrm{ur},1})], \tag{17}$$

$$\sigma_{\mathrm{DE}} = 2\pi \int bdb P_{\mathrm{ur},1} P_{\mathrm{ur},2}, \tag{18}$$

$$\sigma_{\mathrm{SC}} = 2\pi \int bdb[P_{\mathrm{uc},1}(1 - P_{\mathrm{ur},2}) + P_{\mathrm{ur},2}(1 - P_{\mathrm{ur},1})], \tag{19}$$

$$\sigma_{\mathrm{SI}} = 2\pi \int bdb[P_{\mathrm{ui},1}(1 - P_{\mathrm{ur},2}) + P_{\mathrm{ui},2}(1 - P_{\mathrm{ur},1})], \tag{20}$$

$$\sigma_{\mathrm{DC}} = 2\pi \int bdb P_{\mathrm{uc},1} P_{\mathrm{uc},2}, \tag{21}$$

$$\sigma_{\mathrm{DI}} = 2\pi \int bdb P_{\mathrm{ui},1} P_{\mathrm{ui},2}, \tag{22}$$

$$\sigma_{\mathrm{TI}} = 2\pi \int bdb(P_{\mathrm{ui},1} P_{\mathrm{uc},2} + P_{\mathrm{ui},2} P_{\mathrm{ui},1}). \tag{23}$$

As a result of the above calculations, $\sigma_{\mathrm{DE}}/\sigma_{\mathrm{SE}}$ is obtained to be 0.73, which is reasonable because the TE mechanism is not taken into account yet. To pass the TE contribution from double- to SE processes, as shown in Fig. 4 we introduce an equivalent release radius $R'_{r,2}$ for the DE process, which satisfies $\pi R'^2_{r,2} = \pi(R^2_{r,2} - R^2_{\mathrm{TE}})$, that is,

$$R'_{r,2} = \sqrt{R^2_{r,2} - R^2_{\mathrm{TE}}}\ . \tag{24}$$

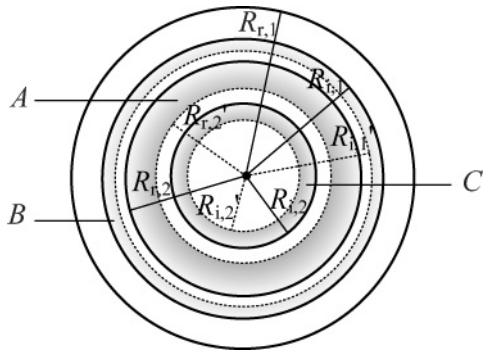


FIG. 4. Equivalent radius diagram. $A = \pi R^2_{\mathrm{TE}}$, $B = \alpha_1 \pi R^2_{\mathrm{TE}}$, and $C = \alpha_2 \pi R^2_{\mathrm{TE}}$.

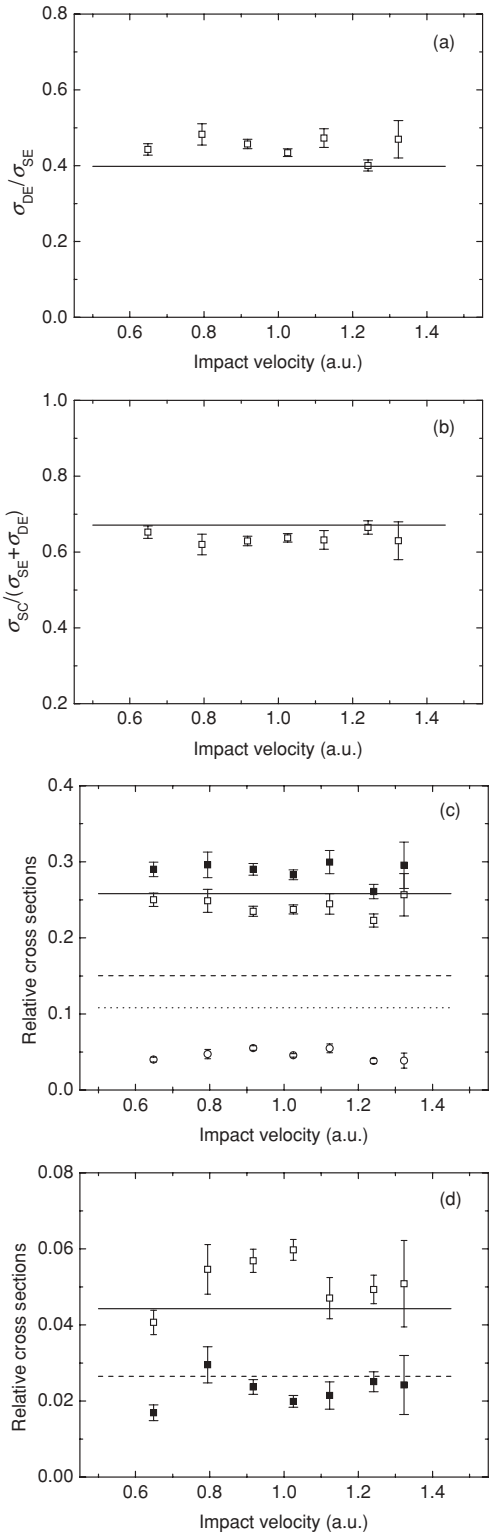


FIG. 5. Our measured relative cross sections for $Xe^{23+}$ + He collisions in comparison with the present estimations. Experiments: (a) $\sigma_{\mathrm{DE}}/\sigma_{\mathrm{SE}}$ (□); (b) $\sigma_{\mathrm{SC}}/(\sigma_{\mathrm{SE}} + \sigma_{\mathrm{DE}})$ (□); (c) $\sigma_{\mathrm{TI}}/(\sigma_{\mathrm{SE}} + \sigma_{\mathrm{DE}})$ (□), $\sigma_{\mathrm{DC}}/(\sigma_{\mathrm{SE}} + \sigma_{\mathrm{DE}})$ (○), $(\sigma_{\mathrm{TI}} + \sigma_{\mathrm{DC}})/(\sigma_{\mathrm{SE}} + \sigma_{\mathrm{DE}})$ (■); (d) $\sigma_{\mathrm{SI}}/(\sigma_{\mathrm{SE}} + \sigma_{\mathrm{DE}})$ (□), $\sigma_{\mathrm{DI}}/(\sigma_{\mathrm{SE}} + \sigma_{\mathrm{DE}})$ (■). Estimations [with $R_{\mathrm{TE}}$ (n→ ∞)]: (a) $\sigma_{\mathrm{DE}}/\sigma_{\mathrm{SE}}$ (solid line); (b) $\sigma_{\mathrm{SC}}/(\sigma_{\mathrm{SE}} + \sigma_{\mathrm{DE}})$ (solid line); (c) $\sigma_{\mathrm{TI}}/(\sigma_{\mathrm{SE}} + \sigma_{\mathrm{DE}})$ (dashed line), $\sigma_{\mathrm{DC}}/(\sigma_{\mathrm{SE}} + \sigma_{\mathrm{DE}})$ (dotted line), $(\sigma_{\mathrm{TI}} + \sigma_{\mathrm{DC}})/(\sigma_{\mathrm{SE}} + \sigma_{\mathrm{DE}})$ (solid line); (d) $\sigma_{\mathrm{SI}}/(\sigma_{\mathrm{SE}} + \sigma_{\mathrm{DE}})$ (solid line), $\sigma_{\mathrm{DI}}/(\sigma_{\mathrm{SE}} + \sigma_{\mathrm{DE}})$ (dashed line).

Equations (8) and (9) can be rewritten as

$$\sigma_{\mathrm{SE}} = \pi\left(R_{r,1}^2 - R_{r,2}'^2\right), \tag{25}$$

$$\sigma_{\mathrm{DE}} = \pi R_{r,2}'^2. \tag{26}$$

Equations (25) and (26) have the same forms with (5) and (6) from the original COB model, respectively. That is, $R'_{r,2}$ is formally equivalent to $R_{r,2}$, but they represent different processes. $\sigma_{\mathrm{SE}}$ in (25) and $\sigma_{\mathrm{DE}}$ in (26) give the net single- and double-electron cross sections, respectively. It can be seen from Fig. 4 that the introduction of $R'_{r,2}$ leads to an increase of the geometric area for net SC by $\pi R_{\mathrm{TE}}^2$, which is supposed to belong to the SC area. We wish to stress here that it seems to be suitable to estimate the value of TE cross section as $\pi R_{\mathrm{TE}}^2$ only when the ionization can be neglected or even is absent at all. However, at the present velocities the ionization at $b < R_{\mathrm{TE}}$ cannot be neglected. It implies that, apart from the TE, a fraction of collisions with $b < R_{\mathrm{TE}}$ will also possibly lead to the ionization of one electron accompanied by the recapture of another to the target which contributes to SC. Thus the TE cross section $\sigma_{\mathrm{TE}}$ should be $\alpha_1 \pi R_{\mathrm{TE}}^2$ where $\alpha_1$ is the proportional coefficient. The value of $\alpha_1$ can be estimated by the ratio of the capture to release distance that the projectile travels at $b < R_{\mathrm{TE}}$. For the first electron $\alpha_1 \approx 1 - R_{i,1}/R_{r,1}$. Therefore, for the first electron we also need to introduce an equivalent ionization radius $R'_{i,1}$ which satisfies $\pi R_{i,1}'^2 = \pi R_{i,1}^2 - \alpha_1 \pi R_{\mathrm{TE}}^2$, that is,

$$R'_{i,1} = \sqrt{R_{i,1}^2 - \alpha_1 R_{\mathrm{TE}}^2}. \tag{27}$$

Similarly, the equivalent ionization radius $R'_{i,2}$ for the second electron is given by

$$R'_{i,2} = \sqrt{R_{i,2}^2 - \alpha_2 R_{\mathrm{TE}}^2}, \tag{28}$$

where $\alpha_2 \approx 1 - R_{i,2}/R_{r,2}$. Then $R_{r,2}$ in (12) and $R_{i,1}$ and $R_{i,2}$ in (13) are replaced by the corresponding equivalent radii $R'_{r,2}$, $R'_{r,1}$, and $R'_{r,2}$, respectively.

The estimated relative cross sections are shown in Figs. 5(a) through 5(d) in comparison with our measurements. As can be seen, agreements are quite satisfactory. The DE process is only about half of the SE process in probability. This is because the DE process only occurs at relatively close collisions and also competes against the SE process, which can occur at either large or small impact parameters. In addition, the DE removal from He followed by the recapture of one of them to the target also contributes to the SE process. In the SE process more than 90% comes from the contribution of SC. The TE mechanism enhances the single-capture cross section, but such a contribution is not as important as that in lower-velocity collisions [17]. This is a result of the attendance of ionization. Due to the highly charged state of the projectile, pure ionization channels are suppressed strongly by capture. Although the sum of DC and TI are well estimated as shown in Fig. 5, the individual DC and TI are significantly overestimated and underestimated, respectively. The reason is the fact that TI partially comes from the autoionization following DC into doubly excited states. However, we simply assume that both electrons are only captured into the ground state. In other words, DC and TI are treated only as the combination of independent-electron events. Therefore, it is not the separate TI or DC cross section, but the sum of them that the present model can estimate reasonably at the present velocities.

## IV. CONCLUSION

In this work, we have measured the cross-section ratios $\sigma_{\mathrm{DE}}/\sigma_{\mathrm{SE}}$, $\sigma_{\mathrm{SC}}/(\sigma_{\mathrm{SE}} + \sigma_{\mathrm{DE}})$, $\sigma_{\mathrm{SI}}/(\sigma_{\mathrm{SE}} + \sigma_{\mathrm{DE}})$, $\sigma_{\mathrm{DI}}/(\sigma_{\mathrm{SE}} + \sigma_{\mathrm{DE}})$, $\sigma_{\mathrm{DC}}/(\sigma_{\mathrm{SE}} + \sigma_{\mathrm{DE}})$, and $\sigma_{\mathrm{TI}}/(\sigma_{\mathrm{SE}} + \sigma_{\mathrm{DE}})$ for $Xe^{23+}$+ He collisions in the velocity range of 0.65–1.32 a.u. In the entire velocity range, the cross-section ratios display weak velocity dependencies. The values of $\sigma_{\mathrm{DE}}/\sigma_{\mathrm{SE}}$, $\sigma_{\mathrm{SC}}/(\sigma_{\mathrm{SE}}+\sigma_{\mathrm{DE}})$, and $\sigma_{\mathrm{TI}}/(\sigma_{\mathrm{SE}} + \sigma_{\mathrm{DE}})$ are about 0.45, 0.63, and 0.24, respectively. Among the processes investigated, pure ionization and DC are the least likely possible. We attempt to apply an extended COB model to reproduce the experimental results. Except for TI and DC, the model provides a good estimation for these relative cross sections. The results show that a fraction of the SE cross section comes from the contribution of the double-electron removal from He accompanied by the recapture of one of these two electrons to the target. However, the contribution from the TE mechanism to SC is less important than that reported in the earlier investigation at lower impact velocities. In addition, although the cross-section ratios $\sigma_{\mathrm{DC}}/(\sigma_{\mathrm{SE}} + \sigma_{\mathrm{DE}})$ and $\sigma_{\mathrm{TI}}/(\sigma_{\mathrm{SE}} + \sigma_{\mathrm{DE}})$ are overestimated and underestimated, respectively, by the present extended classical over-barrier (ECB) model, the sum of these two ratios are in agreement with the estimations, which indicates that DC followed by autoionization is an important mechanism leading to TI.

## ACKNOWLEDGMENTS

The authors would like to express special thanks to Professor Zhihu Yang for his support before and during the experiments. We also thank the staff of the ECRIS Laboratory at the Institute of Modern Physics (IMP), Chinese Academy of Sciences (CAS), for providing a high-quality beam during the course of the experiments. This work is supported, in part, by the National Natural Science Foundation (NSF) of China Grant No. 10704030, by the Fundamental Research Funds for the Central Universities Grant No lzujbky-2010-26, and by the Natural Science Foundation (NSF) of Gansu province Grant No. 0710RJZA014.

[1] C. Illescas and A. Riera, J. Phys. B: At. Mol. Opt. Phys. **31**, 2777 (1998).
[2] H. Ryufuku, K. Saski, and T. Watanabe, Phys. Rev. A **21**, 745 (1980).
[3] A. Niehaus, J. Phys. B: At. Mol. Opt. Phys. **19**, 2925 (1986).
[4] C. F. Maggi, I. D. Horton, and H. P. Summer, Plasma Phys. Control Fusion **42**, 669 (2000).
[5] D. Pequignot, Astron. Astrophys. **81**, 3561 (1980).

[6] H. Andersson, G. Astner, and H. Cederquist, J. Phys. B: At. Mol. Opt. Phys. **21**, L187 (1988).
[7] H. Cederquist *et al.*, J. Phys. B: At. Mol. Opt. Phys. **25**, L69 (1992).
[8] M. Hoshino, T. Kambara, Y. Kanai, R. Schuch, and Y. Yamazaki, Phys. Rev. A **75**, 032722 (2007).
[9] S. Martin, J. Bernard, A. Denis, J. Désesquelles, and L. Chen, Phys. Rev. A **50**, 2322 (1994).
[10] R. Ünal, P. Richard, I. Ben-Itzhak, C. L. Cocke, M. J. Singh, H. Tawara, and N. Woody, Phys. Rev. A **76**, 012710 (2007).
[11] H. Knudsen, H. K. Haugen, and P. Hvelplund, Phys. Rev. A **23**, 597 (1981).
[12] W. Wu, J. P. Giese, I. Ben-Itzhak, C. L. Cocke, P. Richard, M. Stockli, R. Ali, and H. Schöne, Phys. Rev. A **48**, 3617 (1993).
[13] W. Wu, C. L. Cocke, J. P. Giese, F. Melchert, M. L. A. Raphaelian, and M. Stöckli, Phys. Rev. Lett. **75**, 1054 (1995).
[14] D. Y. Yu *et al.*, Phys. Rev. A **76**, 022710 (2007).
[15] B. W. Ding, X. M. Chen, D. Y. Yu, H. B. Fu, G. Z. Sun, and Y. W. Liu, Phys. Rev. A **78**, 062718 (2008).
[16] B. W. Ding *et al.*, Chin. Phys. Lett. **24**, 94 (2007).
[17] H. Cederquist, Phys. Rev. A **43**, 2306 (1991).